Journal of Brilliant Engineering 4 (2025) 41064
Brilliant Engineering
journal home: www.acapublishing.com/journals/4/ben

Research Article

Structural and Optical Characterization of $Zn_{1-x}Co_xO$ Nanoparticles Synthesized via Co-precipitation Method

Sinem KAYAR,[1], Abdulkadir ÖZER*[2]
[1,2] *Atatürk University, Engineering Faculty, Department of Chemical Engineering, Erzurum, Turkey*

Keywords

$Zn_{1-x}Co_xO$,
Nanoparticle,
Co-precipitation method, Co-doping,
Optical properties.

Abstract

$Zn_{1-x}Co_xO$ ($0 \leq x \leq 0.07$) samples have been prepared by the co-precipitation method. The structural and optical properties of Co-doped samples were characterized using XRD, SEM, EDS, XPS, Raman and UV-Visible spectroscopy. XRD, XPS and Raman spectroscopy results show that the ZnO hexagonal wurtzite structure of all samples is preserved and Co^{2+} ions are replaced by Zn^{2+} ions in the ZnO lattice. The average crystallite size of the Zn1-xCoxO nanoparticles were within the range of 25.64–35.86 nm. It was observed that crystal growth increased with increasing Co doping to ZnO. It is seen in SEM images that homogeneously dispersed powders generally have a nanoparticle structure. With the increase of Co concentration, the (Eg) values of Zn1-xCoxO nanoparticles increased from 3.15 to 3.32 eV.

1. Introduction

Zinc oxide (ZnO) has attractive physical and chemical properties. Due to thermal and chemical stability, wide direct band gap energy (3.37 eV) and a large exciton binding energy (60 meV), ZnO is also an interesting material. [1,2]. ZnO are widely used in thermoelectric devices [3], opto-electronic devices [4], sensors [5], light-emitting diodes [6], catalysis [7], solar cells [8], UV protectors [9], varistors [10]. Transition metal doping into ZnO have attracted due to its possible multifunctional device applications. In addition, the optical and electronic properties are improved by doping ZnO with other elements or changing the particle size [11]. The most commonly doped substances in ZnO are Al, Co, Cu, Ni, Mn, Li, etc. [12-17]. Compared to other chemical methods like hydrothermal/solvothermal, sol-gel, aqueous solution deposition, and microemulsion, the co-precipitation method is the most important in the industrial field due to its simplicity, low equipment requirement, high product purity, lower cost, and ability to produce homogeneous nanoparticles [18-21].

In this study, $Zn_{1-x}Co_xO$ ($0 \leq x \leq 0.07$) nanoparticles were synthesized by the co-precipitation method using zinc and cobalt nitrate as precursors, NaOH as a precipitant, and ethanol as a capping agent, and were characterized by structural and optical analysis. Many steel structures such as high-water tanks, water and oil reservoirs, marine structures, and pressure vessels, including shell elements, are widely under stress. Furthermore, shell elements are subject to instability owing to the loads applied. The theoretical buckling resistance (theoretical) is based on a two-branch linear elastic analysis that is suitable for conventional cylinder shells.

2. Experimental Methods

Figure 1 shows the co-precipitation method procedure for the Co doped ZnO samples. 75 ml of purified water and 25 ml of ethanol were charged into a beaker and heated to 50°C with stirring in a heated magnetic stirrer. Required amounts of $Zn(NO_3)_2{\cdot}6H_2O$ and $Co(NO_3)_2{\cdot}6H_2O$ with (x = 0.00, 0.01, 0.03, 0.05 and 0.07) were added to the solution and it was completely dissolved at 600 rpm with continuous stirring. 50 ml of 1 M NaOH solution was added dropwise to the solution to induce precipitation. The pH of the mixture was adjusted around 7-7.5. The mixture was stirred at 50^0C for 1 h. The color of the mixture changed from pink to grayish. The temperature was raised and the mixture was continuous stirred at 80°C for additional 1h. After the precipitation was completed, the mixture was allowed to cool to room temperature. The precipitates were filtered and washed many times with distilled water then dried in a drying oven at 100^0C for 2 h. The dried samples were ground in a mortar and annealed at 500^0C for 2 h under air atmosphere.

The crystal structure of the synthesized samples was examined using X-ray diffraction (XRD) (PANalytical Empyrean). Surface morphology and elemental analysis of the synthesized samples were performed using SEM (Zeiss Sigma 300). Chemical states of elements were done by XPS spectra (Specs-Flex). UV–visible spectra of samples were determined by WITech alpha 300R. Raman spectra of samples were recorded by alpha 300 confocal.

*Corresponding Author: abdulkadirozer04@gmail.com
Received 21 Aug 2025; Revised 22 Aug 2025; Accepted 22 Aug 2025
https://doi.org/10.36937/ben.2025.41064

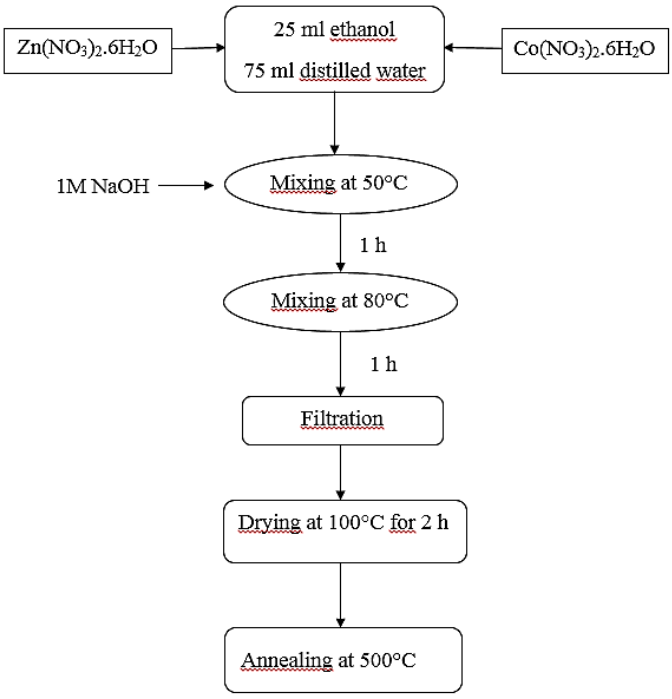

Figure 1. The synthesis process by co-precipitation method

3. Result and Discussion

3.1. Structural and morphological analysis

To investigate the crystal structure of $Zn_{1-x}Co_xO$ ($0 \leq x \leq 0.07$) samples calcined at 500°C for 2 h, the XRD analysis was performed (Figure 2). As shown in Figure 2, the XRD patterns of both pure ZnO and Co-doped samples are all compatible with the standard hexagonal wurtzite structure of ZnO (JCDD 01-080-7099). No additional peaks are observed for x = 0.01 and 0.03 in Co doped ZnO samples. However, very weak additional peaks were detected in the x = 0.05 and 0.07 samples, which may be due to the agglomeration of cobalt atoms at higher doping concentrations. The similarity of the diffraction patterns is attributed to the close match between the ionic radii of Zn^{2+} (0.77 Å) and Co^{2+} (0.76 Å), which helps preserve the phase purity of the Co-doped ZnO samples [22].

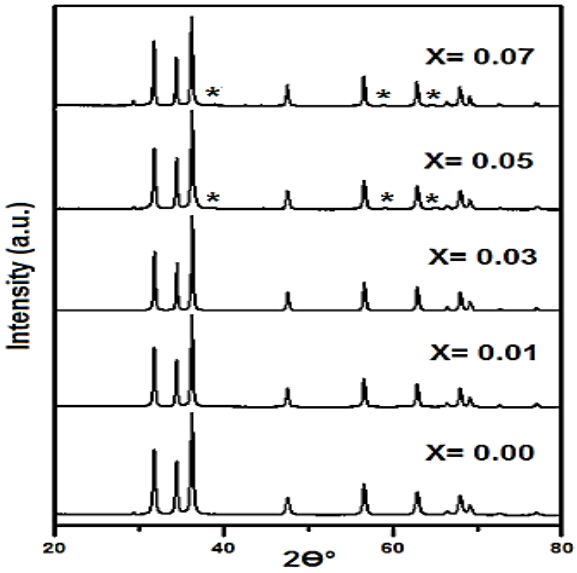

Figure 2. XRD pattern of Co doped ZnO samples

The changes in the peak position (2θ) along the (101) plane is shown in Figure 3. The peak positions are observed to shift to a higher 2θ side (right shift) for x=0.03 and to a lower 2θ side (left shift) for x=0.07. The peak positions are not prominently shifted for x= 0.01 and 0.05. This can be based on the substitution of Co2+ ions in the interstitial position in the ZnO lattice.

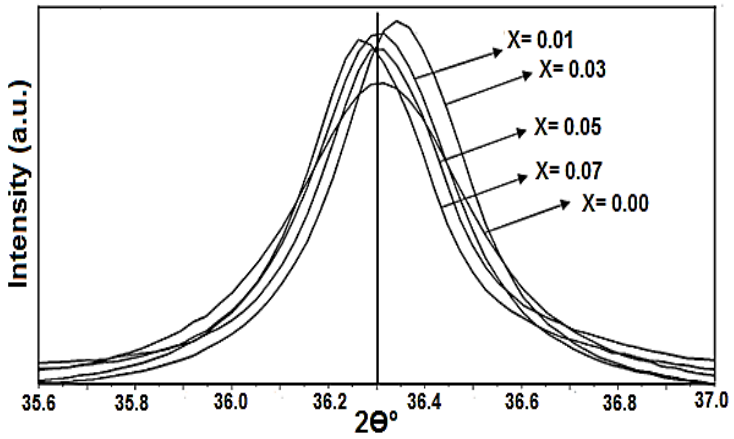

Figure 3. changes in the peak position (2θ) along the (101) plane

The crystallite sizes of samples with different Co doping concentrations ($0 \leq x \leq 0.07$) were calculated using the Scherrer formula [23] and are provided in Table 1. The crystallite size increases from 25.64 nm to 35.86 nm with increase in Co concentration. In higher dopant concentrations, the substitution is affected by chemical thermodynamic limits [24]. The formation of cobalt clusters leads to increase in crystallite size. Conversely, the nucleation of particles increases when a smaller concentration of Co is added to the ZnO sites. These results are consistent with the literature [25,26].

Table 1. The average crystal size (D), 2θ value, FWHM value of $Zn_{1-x}Co_xO$ ($0 \leq x \leq 0.07$) nanoparticles.

Samples	Average crystal size (D) (nm)	2θ (°)	FWHM (β)(°)
X=0.00	25.64	36.311	0.326
X=0.01	32.14	36.308	0.260
X=0.03	34.40	36.346	0.243
X=0.05	35.27	36.309	0.237
X=0.07	35.86	36.275	0.233

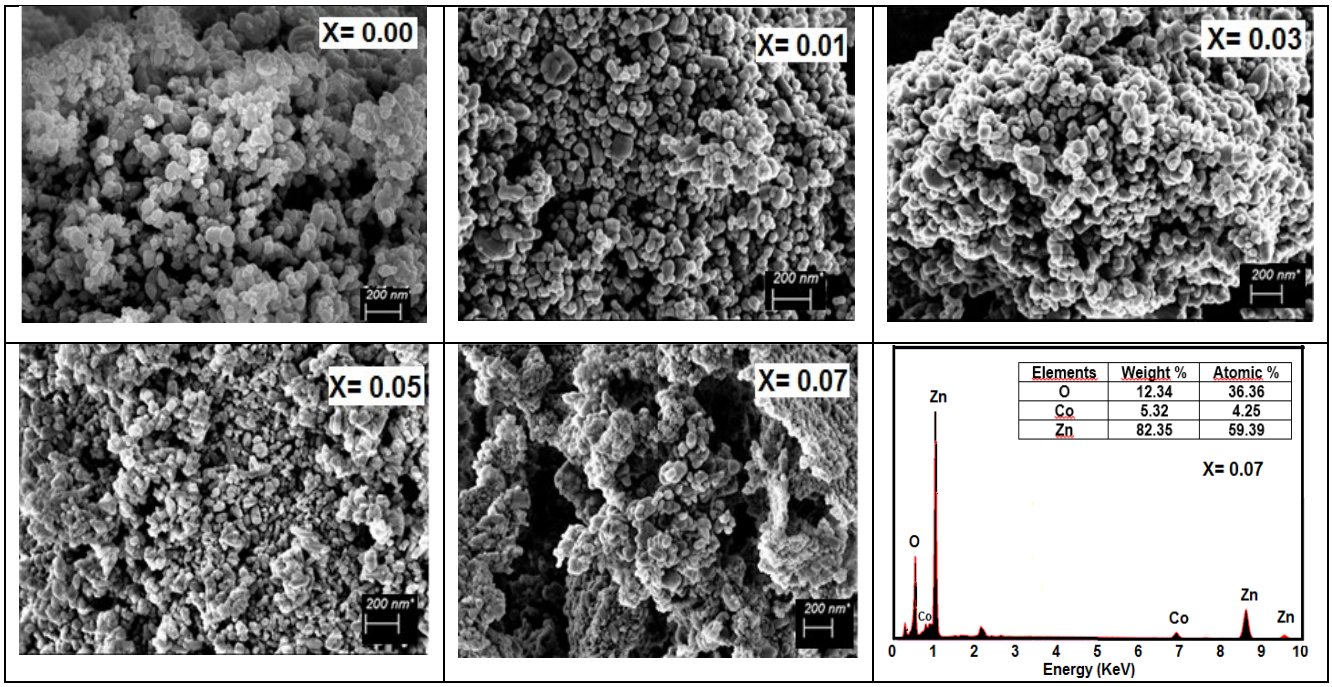

Figure 4. SEM images of Co doped ZnO samples and EDS image of $Zn_{0.93}Co_{0.07}O$

The morphology of the synthesized samples was examined by SEM combined with EDS. SEM images of the ZnO undoped and doped with various concentration of Co (i.e., x= 0.0, 0.01, 0.03, 0.05, and 0.07) annealed at 500°C for two hours are given in Figure 4. SEM analysis show that the all samples consist of dense, spherical like particles randomly arranged and agglomeration. The average particle size was found to increase with the increase of Co doping in the ZnO particles. This is in agreement with the particle size results calculated using the Scherrer equation. The EDS spectrum detected only the presence of Co, Zn, and O atoms, with no other unknown impurities.

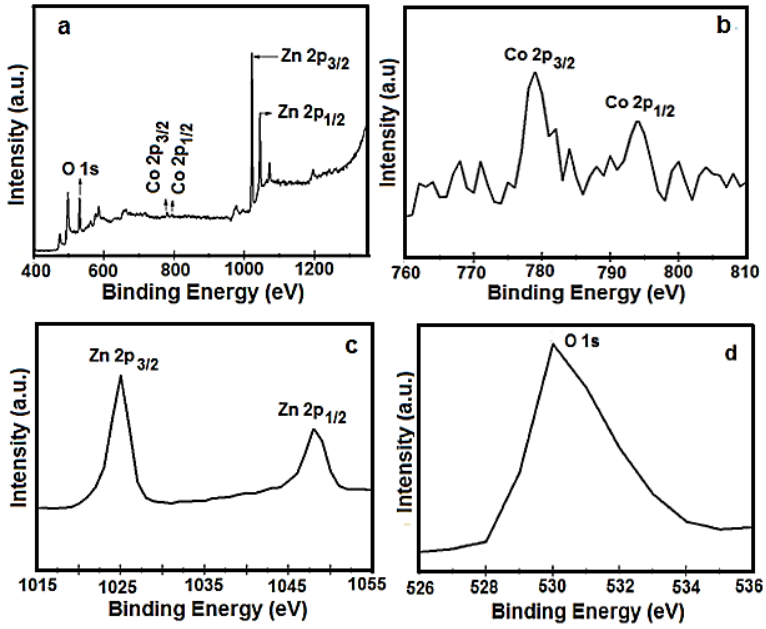

Figure 5. XPS spectra of $Zn_{0.95}Co_5O$ nanoparticles: the full-spectrum (a), Zn 2p (b), Co 2p (c), and O 1s (d).

The presence of Co and its oxidation state in $Zn_{0.93}Co_{0.07}O$ nanoparticles were determined by XPS analysis. As seen in Figure 5a, the characteristic peaks correspond only to Zn, Co, and O. A high-resolution scan of Co 2p identifies the exact peak locations for Co $2p^{3/2}$ and Co $2p^{1/2}$ at 778.9 eV and 794.0 eV, respectively (Figure 5b). This indicates that the dopant atoms are well-incorporated into the Zn-lattice sites. Two strong peaks at 1022.9 and 1044.1 eV in the Zn 2p spectrum are identified as Zn $2p^{3/2}$ and Zn $2p^{1/2}$, respectively, supporting that Zn is present as Zn^{2+} (Figure 5c). The binding energy of O 1s, obtained at 530.0 eV, corresponds to O^{2-} ions in the ZnO lattice (Figure 5d). These results agree with the data in the literature on Co^{+2} in $Zn_{1-x}Co_xO$ [27-30].

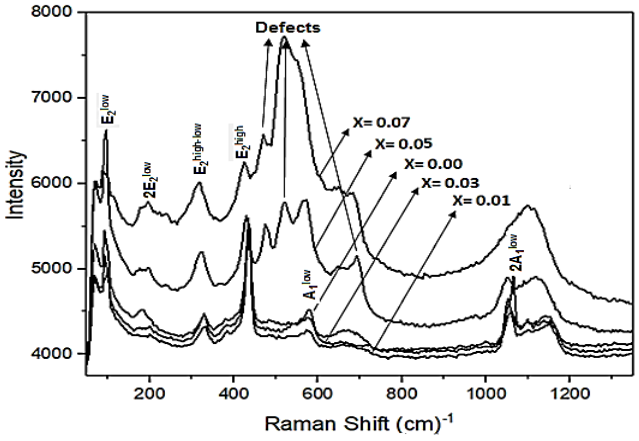

Figure 6. Raman spectra of samples

As observed from Figure 6, the Raman spectra of all samples show E_2^{high} and E_2^{low}, which are the characteristic phonon vibrations of ZnO at 437 and 97 cm^{-1} originating from the O and Zn sublattices, respectively. The oxygen sublattice vibration optical mode (E2high) was shifted toward lower frequency (425 cm^{-1}) compared to ZnO nanoparticle. The spectra also showed the first and second order multiphonon scattering vibrations at 184, 331, 665 and 1067 cm^{-1} depending on $2E_2^{low}$, $E_2^{high-low}$, A_1^{low} and $2A_1^{low}$, respectively [31]. Additionally, it is observed that the peaks at 471, 520 and 694 cm^{-1}, which are defect-induced modes, appear at higher Co concentrations (x=0.05 and 0.07) and the intensity of the defect peaks increases with the increase in concentration.

3.2. Optical properties

The band gap of $Zn_{1-x}Co_xO$ nanoparticles was investigated by UV-Visible diffuse reflection spectroscopy. The optical absorption spectra of the synthesized samples are shown in Figure 7. When the spectra of Co-doped samples were compared to that of pure ZnO, three distinct peaks were detected at 565, 612, and 656 nm. These peaks represent the transitions 4A2(F)→2A1(G), 4A2(F)→4T1(P), and 4A2(F)→2E(G). In order to determine the optical band gap (Eg) values of undoped and Co doped ZnO samples, the optical data have been calculated by using Tauc Eq. (1) [33].

$$\alpha h\nu^2 = A\,(h\nu - Eg)^n \quad (1)$$

Since ZnO has a direct band transition, the n value was taken as 1/2. The (Eg) values for $Zn_{1-x}Co_xO$ nanoparticles were determined from their absorbance spectra by extrapolating the linear region of the $(\alpha h\nu)^2$ plot versus ($h\nu$). With the increase of Co concentration, the (Eg) values of Co-doped ZnO samples increased from 3.15 to 3.32 eV (Figure 8). Similar observations for Co-doped ZnO are also given in the literature. [34,35].

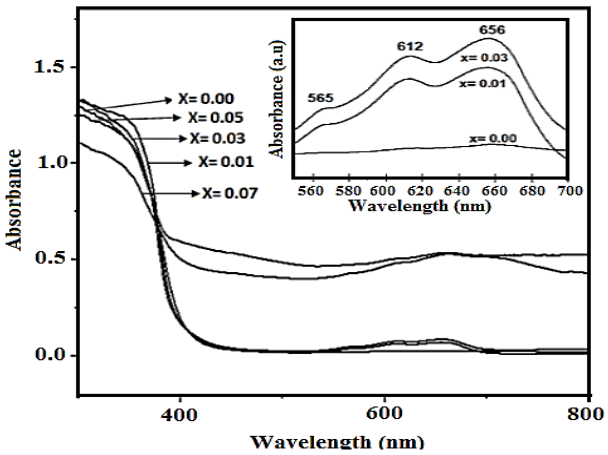

Figure 7. UV–Visible absorption spectra of samples

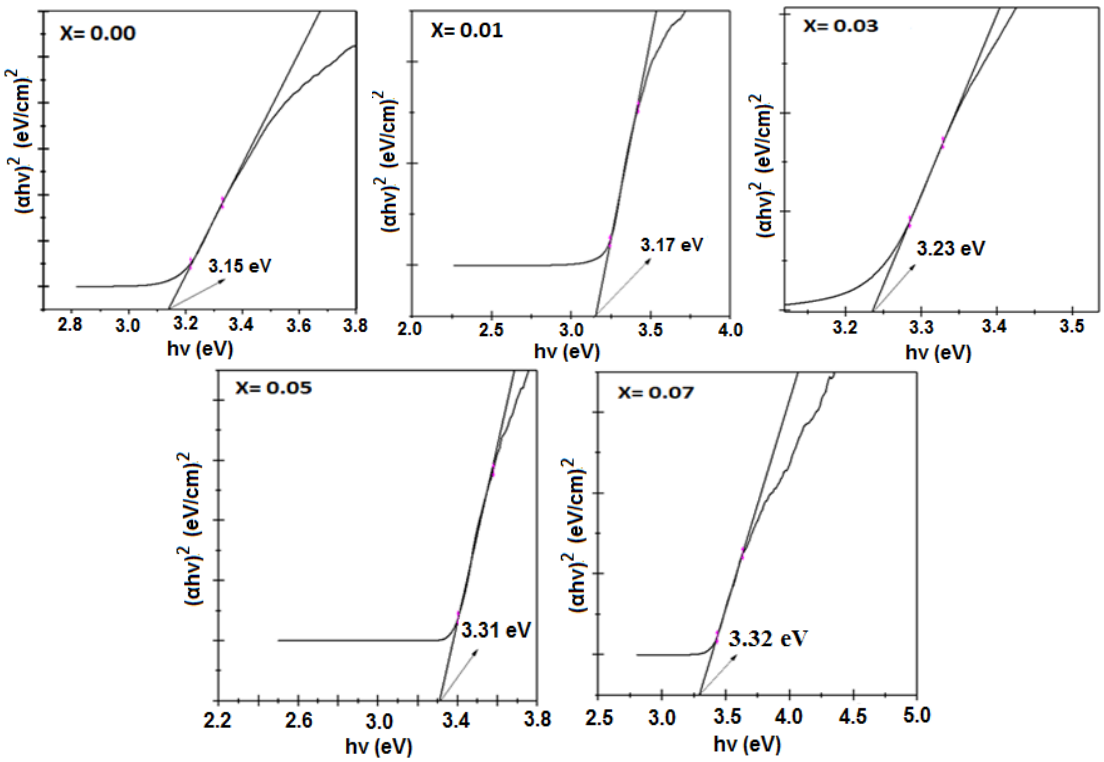

Figure 8. Optical band gap (Eg) values of synthesized samples

4. Conclusion

$Zn_{1-x}Co_xO$ (x=0.00-0.07) nanoparticles were synthesized using the co-precipitation method. The structural and optical properties of the synthesized samples are examined using various characterization techniques. The XRD patterns exhibit that the crystal size was found to increase with the increase in Co content. SEM micrographs indicates the formation of particle shaped nanostructures at all samples. According to XPS and Raman spectroscopy results, it is seen that Co addition does not affect the wurtzite structure of ZnO. It was shown that cobalt ions incorporated into the ZnO matrix. The Eg increases from 3.15 eV to 3.32 eV with Co doping. All band gap values for the Co-doped samples are higher when compared to bulk ZnO (3.15 eV). The obtained results showed that Co doped ZnO nanoparticles are a good candidate for the optoelectronic devices.

Declaration of Conflict of Interests

The authors declare that there is no conflict of interest. They have no known competing financial interests or personal relationships that could have appeared to influence the work reported in this paper.

References

[1.] Sedky, A., Afify, N., Almohammedi, A., Ibrahim, E. M. M., & Ali, A. M. (2023). Structural, optical, photoluminescence and magnetic investigation of doped and Co-doped ZnO nanoparticles. Optical and Quantum Electronics, 55(5), 456.

[2.] Kammoun, S., & Ghoul, J. E. (2021). Structural and optical investigation of Co-doped ZnO nanoparticles for nanooptoelectronic devices. Journal of Materials Science: Materials in Electronics, 32(6), 7215-7225.

[3.] Ali, H. T., Jacob, J., Khalid, M., Mahmood, K., Yusuf, M., Mehboob, K., & Ashar, A. (2021). Optimizing the structural, morphological and thermoelectric properties of zinc oxide by the modulation of cobalt doping concentration. Journal of Alloys and Compounds, 871, 159564.

[4.] Kumar, P. S., Johnson, J., & Biju, C. S. (2024). Structural, morphological, and optoelectronic characteristics of Zn, Cd-co-doped CuO nanostructures. Journal of Materials Science: Materials in Electronics, 35(18), 1233.

[5.] Himabindu, B., Devi, N. L., Nagaraju, P., & Kanth, B. R. (2024). Synthesis and characterization of flower-like cobalt-doped ZnO nanostructures for ammonia sensing applications. ECS Journal of Solid State Science and Technology, 13(2), 027006.

[6.] Chen, L., Zhang, Y., Kun, Y., Tuo, K., Shang, J., Du, W., & Liu, S. (2024). The Zn1−xMgxO electron transport layer for charge balance in high-brightness inverted quantum-dot light-emitting diodes. Journal of Materials Science: Materials in Electronics, 35(11), 754.

[7.] Yimer, S. M., & Melaku, A. Z. (2025). Bio-inspired synthesis of Co-doped CuO/ZnO nanocomposites for enhanced photocatalytic degradation of methyl blue. Results in Chemistry, 102535.

[8.] Archi, M., Moulaoui, L., Karouchi, M., Darkaoui, E., Laassouli, A., Bajjou, O., ... & Elhadadi, B. (2025). First-principles study of co-doped wurtzite ZnO: insights into carrier dynamics, visible light absorption, and structural properties for solar cell applications. Optical and Quantum Electronics, 57(5), 269.

[9.] Kumar, P., Kaushal, S., Kumar, S., Dalal, J., Batoo, K. M., & Ahlawat, D. S. (2025). Recent advancements in pure and doped zinc oxide nanostructures for UV photodetectors application. Physica B: Condensed Matter, 417177.

[10.] Kelleher, M. (2024). ZnO varistors—Preparation of nano and micro sized powders by mechanical methods for low and high voltage varistors.

[11.] Singh, S., Gade, J. V., Verma, D. K., Elyor, B., & Jain, B. (2024). Exploring ZnO nanoparticles: UV–visible analysis and different size estimation methods. Optical Materials, 152, 115422.

[12.] Liao, Y. D., Huang, P. C., Lin, Y. C., & Xu, L. (2025). Aluminum-doped Zinc Oxide Prepared by Selective Laser Sintering of Nanoparticles for Thermoelectric Application. Ceramics International.

[13.] Goswami, N., & Jha, R. K. (2025). Structural, thermal and dielectric studies of cobalt doped ZnO nanoparticles prepared by chemical precipitation method. Journal of Molecular Structure, 1326, 141063.

[14.] Behfar, S., Ghorbanpour, M., & Alatabe, M. J. A. (2025). Characterisation and visible light induced antibacterial activity of Cu-doped zinc oxide nanoparticles. Indian Chemical Engineer, 1-10.

[15.] Fawad, M., Maqsood, N., Nawaz, A., Islam, B., Zaheer, M. D., & Skotnicová, K. (2025). Synthesis, characterization, and enhanced optical and dielectric properties of pure and Ni-doped ZnO nanoparticles for advanced electronic applications. Results in Engineering, 26, 104824.

[16.] Andiyappan, K., & Ramalingam, S. (2025). Green synthesis of manganese (Mn) doped zinc oxide (ZnO) nano-additives from biodegradable novel dragon fruit peel extracts and its effect on reactivity controlled compression ignition (RCCI) engine performance. Energy, 324, 135936.

[17.] Shestakov, M. V., Gippius, A. A., & Baranov, A. N. (2025). Structural Research of Li Doped ZnO Powders. Journal of Structural Chemistry, 66(2), 386-398.

[18.] Abbas, A. K., AL-Jawad, S. M., & Imran, N. J. (2025). Antibacterial Activity of Undoped and (Zn, Co) Co-Doped CuO Nanostructure Prepared by Hydrothermal Technique. Plasmonics, 1-17.

[19.] Li, Z., Li, Y., Song, G., & Wang, R. (2025). Enhanced triethylamine sensing performance of Co-doped ZnO nanorods prepared using a solvothermal method. Transactions of Materials Research, 100080.

[20.] Pandey, K., Kumar, M., Chauhan, S., & Raman, R. S. (2025). Microwave-assisted sol-gel synthesis of Li-Co doped zinc oxide nanoparticles: Investigating the effects of codoping on structural, optical, and magnetic properties for spintronic applications. Journal of Crystal Growth, 652, 128053.

[21.] Feng, Y., Zhao, L., Zou, Y., Liu, Z., Xiao, P., Wei, D., ... & Tang, X. (2025). Thermosensitive microemulsion gel incorporating nano-ZnO and black soybean tar improves treatment adherence and alleviates psoriasis-like skin disease. Colloids and Surfaces B: Biointerfaces, 114812.

[22.] Naik, E. I., Naik, H. B., Sarvajith, M. S., & Pradeepa, E. (2021). Co-precipitation synthesis of cobalt doped ZnO nanoparticles: Characterization and their applications for biosensing and antibacterial studies. Inorganic Chemistry Communications, 130, 108678.

[23.] Klug, H. P., Alexander, L . E., (1974). X-ray diffraction procedures: for polycrystalline and amorphous materials. X-Ray Diffraction Procedures: For Polycrystalline and Amorphous Materials, 2nd Edition, by Harold P. Klug, Leroy E. Alexander, Wiley-VCH, pp 992.

[24.] Hareeshanaik, S., Prabhakara, M. C., Naik, H. B., Viswanath, R., Shivaraj, B., Vishnu, G., & Adarshgowda, N. (2023). Optical, photo catalytic, electrochemical and antibacterial performance of ZnO and Co doped ZnO nanoparticles. Inorganic Chemistry Communications, 158, 111552.

[25.] Shishodia, P. K., (2016). Effect of cobalt doping on ZnO thin films deposited by sol-gel method, Thin Solid Films, 612, 55-60.

[26.] Dutta, A., Chatterjee, K., Mishra, S., Saha, S. K., & Akhtar, A. J. (2022). An insight into the electrochemical performance of cobalt-doped ZnO quantum dot for supercapacitor applications. Journal of Materials Research, 37(22), 3955-3964.

[27.] Yan, H., Xue, J., Chen, W., Tang, J., Zhong, L., Zhou, T., & Zhao, X. (2021). Optimizing physical properties of Co-doped ZnO nanoparticles: Controlling oxygen vacancy and carrier concentration. Vacuum, 192, 110488.

[28.] Ali, H. T., Jacob, J., Khalid, M., Mahmood, K., Yusuf, M., Mehboob, K., ... & Ashar, A. (2021). Optimizing the structural, morphological and thermoelectric properties of zinc oxide by the modulation of cobalt doping concentration. Journal of Alloys and Compounds, 871, 159564.

[29.] Saadi, H., Khaldi, O., Pina, J., Costa, T., Seixas de Melo, J. S., Vilarinho, P., & Benzarti, Z. (2024). Effect of Co doping on the physical properties and organic pollutant photodegradation efficiency of ZnO nanoparticles for environmental applications. Nanomaterials, 14(1), 122.

[30.] Cheng, K., Cao, D., Yang, F., Xu, Y., Sun, G., Ye, K., & Wang, G. (2014). Facile synthesis of morphology-controlled Co3O4 nanostructures through solvothermal method with enhanced catalytic activity for H2O2 electro reduction, J. Power Sources 253, 214-223.

[31.] Karpyna, V., Myroniuk, L., Myroniuk, D., Bykov, O., Olifan, O., Kolomys, O., ... & Ievtushenko, A. (2024). Effect of cobalt doping on structural, optical, and photocatalytic properties of ZnO nanostructures. Catalysis Letters, 154(5), 2503-2512.

[32.] Buzok, E. B., Yalcin, S., Demircan, G., Yılmaz, D., Aktas, B., & Aytar, E. (2024). The structural, optical, electrical and radiation shielding properties of Co-doped ZnO thin films. Radiation Physics and Chemistry, 222, 111840.

[33.] Tauc, J., Grigorovici, R., & Vancu, A. (1966). Optical Properties and Electronic Structure of Amorphous Germanium, Phys. Status Solidi (b), 15, 627-637.

[34.] Murtaza, G., Abbas, Y., & Ahmed, F. (2025). Theoretical and experimental study of structural, electronic and optical properties of cobalt-doped zinc oxide. Physica B: Condensed Matter, 417283.

[35.] Guzman, M. L. T., Aguilar, C. J., Lópera, W., Diosa, J. E., & Mosquera-Vargas, E. (2024). Influence of cobalt doping on structural, optical, and electrical properties of zinc oxide nanoparticles prepared by polymeric precursor method. Optical Materials, 154, 115753.

How to Cite This Article

Kayar, S., and Özer, A. K., Structural and Optical Characterization of $Zn_{1-x}Co_xO$ Nanoparticles Synthesized via Co-Precipitation Method, Brilliant Engineering, 4(2025),41064.
https://doi.org/10.36937/ben.2025.41064